

Supporting Information for

Au-Cu Alloy Bridged Synthesis and Optoelectronic Properties of Au@CuInSe₂ Core-Shell Hybrid Nanostructures

Qingfeng Zhang,^a Jianjun Wang,^b Zhiyuan Jiang,^{*a} Yu-Guo Guo,^b Li-Jun Wan,^b
Zhaoxiong Xie^a and Lansun Zheng^a

^aState Key Laboratory for Physical Chemistry of Solid Surfaces and Department of Chemistry, College of Chemistry and Chemical Engineering, Xiamen University, Xiamen, Fujian 361005, P. R. China.

^bCAS Key Laboratory of Molecular Nanostructure and Nanotechnology and Beijing National Laboratory for Molecular Sciences, Institute of Chemistry, Chinese Academy of Sciences, Beijing 100190, P. R. China.

E-mail: zyjiang@xmu.edu.cn

Experimental Section

Chemicals and Material: Copper (I) chloride (CuCl, 99%), Indium (III) chloride (InCl₃, anhydrous 99.99%) and Selenium powder (Se, 99.999%) were purchased from Alfa Aesar. Oleylamine (C18-content: 80-90%) was purchased from ACROS. Toluene, 1, 2-dichlorobenzene and P3HT (Mn, 20000, Mw, 33000) were A.R. grade bought from the Beijing Chemical Factory, China. Chloroauric acid (HAuCl₄•4H₂O), Triphenylphosphine (C₁₈H₁₅P), Anhydrous ethanol and chloroform were purchased from Sinopharm Chemical Reagent Co. Ltd. (Shanghai, China). Above chemicals were used as received without further purification. AuPPh₃Cl was synthesized by reacting HAuCl₄•4H₂O with C₁₈H₁₅P in ethanol.¹ Copper (I) chloride and Indium (III) chloride were stored in a nitrogen-filled glovebox to prevent oxidization and degradation.

Synthesis of Au@CuInSe₂ Nanostructure: All syntheses were carried out using a Schlenk line. Typically, Au NPs were prepared by adding 32 mg of AuPPh₃Cl and 5 mL of oleylamine into a 50 mL three-neck flask and the reaction was carried out at 130 °C for 30 min. At the same time, 0.0125 g (0.0125 mM) of CuCl, 0.0275 g (0.0125 mM) of InCl₃ and 5 mL of oleylamine were loaded in a 50 mL three-neck flask under air-free condition. The mixture was heated to 130 °C and

kept at 130 °C for 30 min. The color changed from blue to yellow indicated the formation of oleylamine complexes with Cu (I) and In (III). Meanwhile, in order to dissolving selenium powder in oleylamine, 20 mg (0.025 mM) of selenium powder were added to 10 mL of oleylamine in a 50 mL three-neck flask and the mixture were heated to 180 °C and held for 60 min, the color changed from black, to brown, and finally brownish red due to dissolution of selenium powder in oleylamine. After that, the Cu (I) and In (III) oleylamine complexes were injected into the Au NPs solution and heated rapidly to 260 °C. Then the Se-oleylamine solution was immediately injected into the above solution and the reaction mixture was kept at 260 °C for 30 minutes. Finally, the reaction mixture was cooled down to the room temperature followed by purification of nanoparticles. The resulting Au@CuInSe₂ nanoparticles form stable suspensions in organic solvents, such as chloroform and toluene.

Fabrication of Photodetector Device: P3HT (75 mg) was dissolved in 5 mL 1, 2-dichlorobenzene. 100 μL nanocrystals solution and 200 μL P3HT solution was mixed to form the final solution. The device was fabricated by dropping 1 μL of solution onto precleaned platinum electrodes and drying in air. The device was measured in air.

Characterization: X-ray diffraction measurements were performed on PANalytical X-Pert diffractometer with Cu K α radiation. The morphology and structure of the products were investigated using scanning electron microscopy (SEM, HITACHI S-4800) and transmission electron microscopy (TEM, FEI Tecnai-F30 FEG). The composition of the nanocrystals was analyzed by energy dispersive X-ray spectrometry (EDX) using EDX system built on a HITACHI S-4800 SEM. Line profiles were performed with an EDX system attached to a Tecnai-F30 TEM. X-ray photoelectron spectra (XPS) and the Auger Electron Spectroscopy (AES) spectra were acquired on a PHI Quantum-2000. UV-vis absorption spectra were recorded at room temperature with a Lambda 950 UV-vis spectrometer and a Varian Carry-5000 UV-Vis-NIR spectrometer. The PL spectra were record on a Hitachi F-7000. Current-voltage (I-V) characteristics of the devices were recorded with a Keithley 4200 SCS and a Micromanipulator 6150 probe station in a shielded and clean box at room temperature. An iodine-tungsten lamp was selected as a white light source.

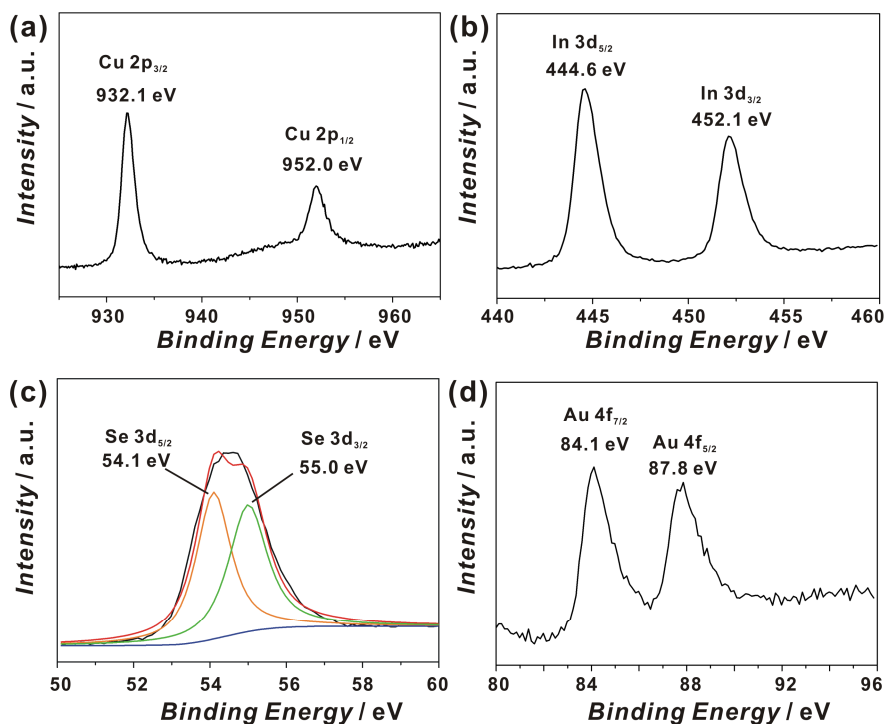


Figure S1. High-resolution XPS spectra of Cu 2p, In 3d, Se 3d and Au 4f regions taken of Au@CuInSe₂ nanostructures.

The elemental oxidation states of chemical composites of the Au@CuInSe₂ were investigated by XPS. The Cu 2p_{3/2} peak at 932.1 eV matches well with the reported binding energy for Cu⁺ in CuInSe₂, and we can confirm that no Cu²⁺ exists because the binding energy of Cu²⁺ should be centered at 942.0 eV, which was not observed in the XPS spectrum (Figure S1a). Besides, the In 3d_{5/2} peak at 444.6 eV (Figure S1b) is representative of In³⁺ in CuInSe₂, while the Se 3d_{5/2} peak at 54.1 eV (Figure S1c) is representative of the Se 3d binding energy for lattice Se²⁻, the Au 4f_{7/2} peak at 84.1 eV (Figure S1d) is in agreement with that of Au⁰ reported in literature.²

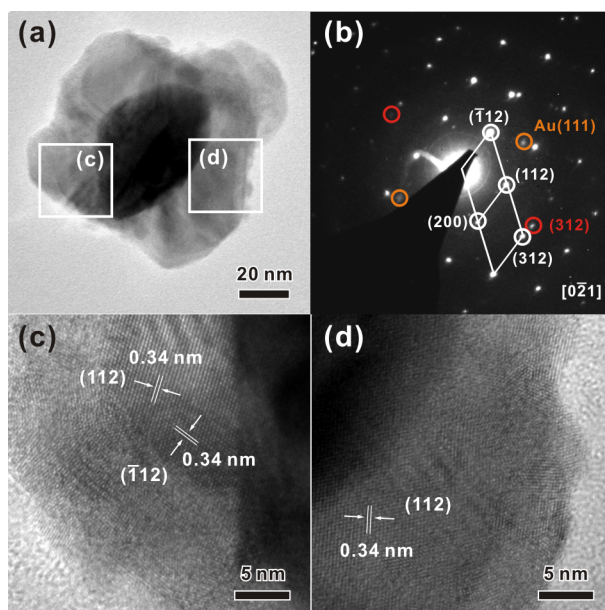


Figure S2. (a) Typical TEM image and (b) Corresponding SAED pattern of an individual Au@CuInSe₂ core-shell nanostructure; (c), (d) HRTEM images recorded in the area marked in (a).

The structural features of the as-prepared NPs were revealed by TEM images and SAED patterns. The contrast between the core and the shell of the NPs was easily distinguishable in the TEM images as shown in Figure S2. It can be obviously observed from Figure S2a that the CuInSe₂ shell contains multiple crystal domains. Figure S2b shows the corresponding SAED pattern of the individual nanostructure, a few spots (marked by orange cycle) were caused by the Au core, one set of the reflections (marked with white cycles) can be indexed as tetragonal chalcopyrite CuInSe₂ with $[0\bar{2}1]$ zone axis. Some additional diffraction spots (marked by red cycle) were caused by CuInSe₂ nanocrystal with other orientation. The interlayer spacing of 0.34 nm observed in the shell region (Figure S2c, S2d) comply with the lattice planes of (112) and $(\bar{1}12)$ of CuInSe₂, there is distinct deviation between the directions of (112) in the Figure S2c and Figure S2d, confirming that each CuInSe₂ nanocrystal adopted different orientation. These results proved that the shell contains multiple crystal domains. No obvious epitaxial relationship between Au core and CuInSe₂ shell can be found even tens of single hybrid nanostructures have been investigated in the TEM.

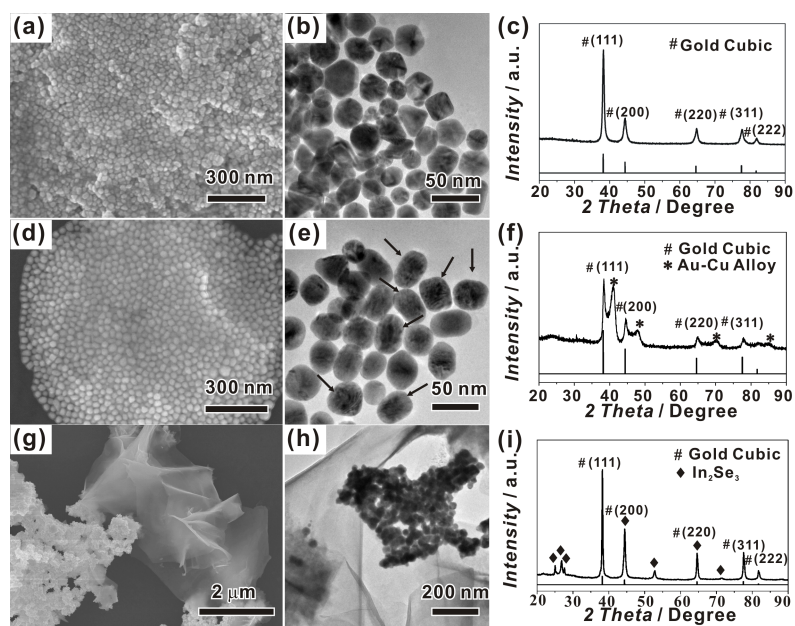


Figure S3. (a) typical SEM image, (b) TEM image and (c) XRD pattern of the preformed Au NPs; (d) SEM image, (e) TEM image and (f) XRD pattern of the products without adding the Se source; (g) SEM image, (h) TEM image and (i) XRD pattern of the products in the absence of CuCl in the reaction.

Figure S3a-S3c show the morphology and phase of Au NPs prepared in oleylamine at 130 °C. The size of the Au NPs is in the range of 20-40 nm and most of the Au NPs have a Five-fold twined structure. The XRD pattern matches well with the fcc Au (JCPDS No.04-0784) and no impurity was found among the products. Figure S3d-S3f reveals the structure information of the product obtained when the reaction was quenched at 260 °C without adding the Se source. Complex Moiré fringes can be observed from the TEM image as marked by the arrow, indicating the formation of Au-Cu alloy thin layer on the surface of the Au NPs when Cu atoms are alloyed into the crystal lattice. The existence of the core-shell structure can also be confirmed by the XRD pattern which shows two different phases that can be attributed to fcc Au and Au-Cu alloy respectively. It was also demonstrated that only separated Au NPs and In₂Se₃ flakes can be obtained in the absence of CuCl in the reaction (Figure S3g-S3i). No core-shell structure was observed verifies the phase separation of Au and In₂Se₃.

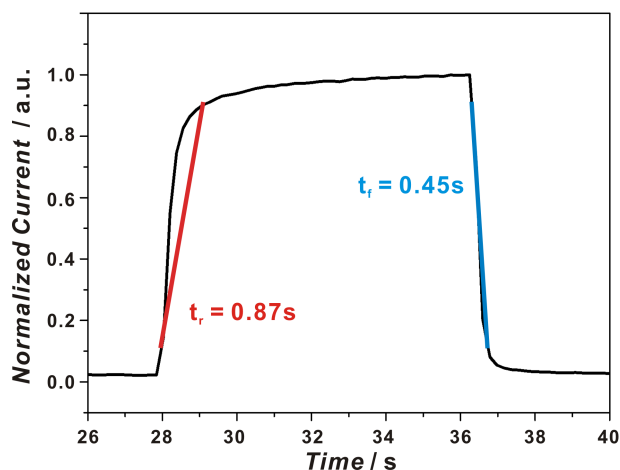


Figure S4. A single normalized cycle of On/Off switching of the hybrid device of Au@CuInSe₂ nanostructures measured at an incident density of 7.63 mW cm⁻² and bias voltage of 1 V.

In Figure S4, the red and blue lines highlight the leading and trailing edges. The measured response time, defined as the time required for photocurrent increasing from 10% I_{peak} to 90% I_{peak} is 0.87 s. Similarly, the recovery time, which is the time for photocurrent decreasing from 90% I_{peak} to 10% I_{peak} , is 0.45 s.

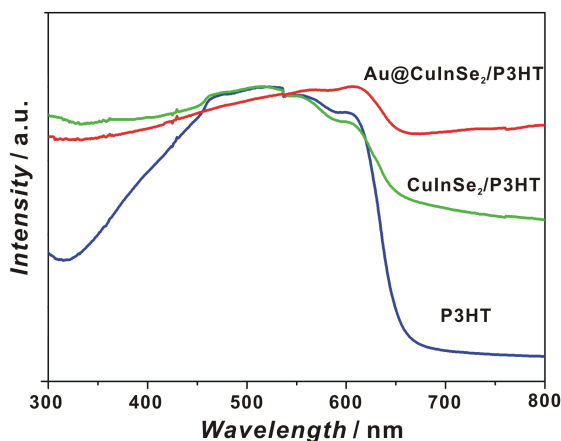


Figure S5. UV-vis spectra of the P3HT film (blue), CuInSe₂/P3HT hybrid film (green) and Au@CuInSe₂/P3HT hybrid film (red).

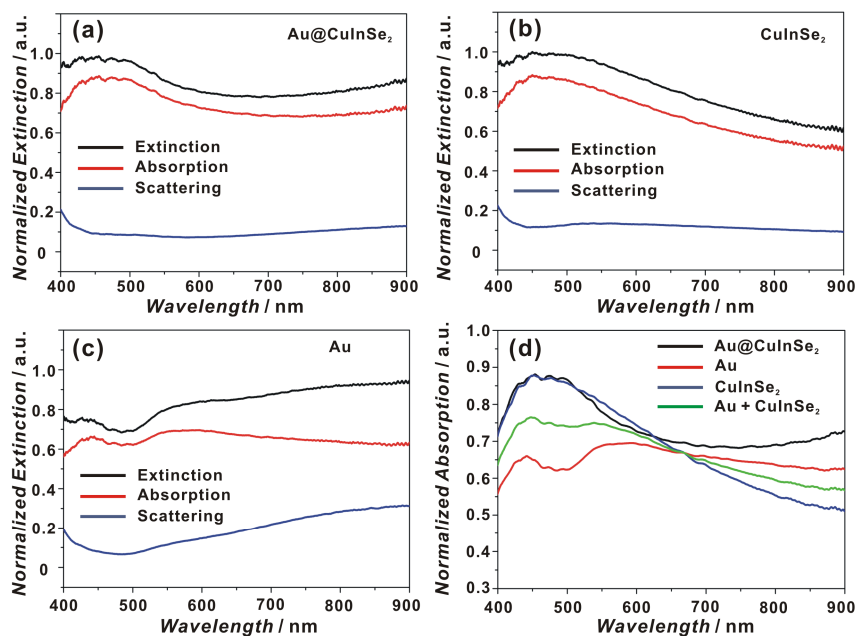


Figure S6. (a), (b), (c) Correction of the UV-vis spectrums of Au@CuInSe₂, CuInSe₂ and Au NPs, respectively; (d) Correctional UV-vis absorption spectra of Au@CuInSe₂ nanostructures, Au NPs, CuInSe₂ NPs, the mixture of Au NPs and CuInSe₂ NPs. In these experiments, the size of Au NPs is in the range of 30-50 nm, which is close to the size of the Au core in the Au@CuInSe₂ nanostructures; the size of the CuInSe₂ NPs is in the range of 80-130 nm, which is close to the size of Au@CuInSe₂ nanostructures. All of the solutions were with the same concentration.

To clarify whether enhanced absorption occurs in Au@CuInSe₂ NPs, the amount of absorption in an extinction spectrum was estimated via a reported correction method.³ The extinction spectra of Au NPs, CuInSe₂ NPs and Au@CuInSe₂ ethanol solution were measured by a spectrophotometer, the scattering spectra were measured by a spectrofluorimeter. Then the extinction spectra were separated into absorption and scattering components via simulation. Figure S6a-S6c showed the correctional extinction spectra (black line) and their absorption component (red line)/scattering component (blue line), which indicated that the absorption is the dominant factor in the extinction of as-prepared NPs. The Au NPs has a wide SPR absorption peak at ~ 570 nm, which could be attributed to the size of Au NPs (30-50 nm). Figure S6d is the correctional absorption spectra which demonstrate that the Au@CuInSe₂ nanostructures obviously enhance the absorption in the range of 650-900 nm in comparison to CuInSe₂ NPs, Au NPs, as well as the mixture of the CuInSe₂ NPs and Au NPs.

Reference:

- 1 P. Braunstein, H. Lehner and D. Matt, *Inorg. Synth.* 1990, **27**, 218.
- 2 C. D. Wagner, in *Practical Surface Analysis*, ed. D. Briggs and M. P. Seah, John Wiley and Sons, 2nd edn., **1990**, Vol. 1, pp. 595-634.
- 3 N. Micali, F. Mallamace, M. Castriano, A. Romeo, L. M. Scolaro, *Anal. Chem.*, **2001**, *73*, 4958.